J Biochem 127, 861–869 (2000)

Irreversible Conformational Change of Bacterio-opsin Induced by Binding of Retinal during Its Reconstitution to Bacteriorhodopsin, as Studied by ^{13}C NMR[1]

Satoru Yamaguchi,* Satoru Tuzi,* Michikazu Tanio,* Akira Naito,* Janos K. Lanyi,† Richard Needleman,‡ and Hazime Saitô*,[2]

Department of Life Science, Faculty of Science, Himeji Institute of Technology, Harima Science Garden City, Kouto 3-chome, Kamigori, Hyogo 678-1297, and †Department of Biophysics and Physiology, University of California, Irvine, California 92697, USA, and ‡Department of Biochemistry, Wayne State University, Detroit, Michigan 48201, USA

Received December 16, 1999; accepted February 24, 2000

We compared ^{13}C NMR spectra of [3-^{13}C]Ala- and [1-^{13}C]Val-labeled bacterio-opsin (bO), produced either by bleaching bR with hydroxylamine or from a retinal-deficient strain, with those of bacteriorhodopsin (bR), in order to gain insight into the conformational changes of the protein backbone that lead to correct folding after retinal is added to bO. The observed ^{13}C NMR spectrum of bO produced by bleaching is not greatly different from that of bR, except for the presence of suppressed or decreased peak-intensities. From careful evaluation of the intensity differences between cross polarization magic angle spinning (CP-MAS) and dipolar decoupled–magic angle spinning (DD-MAS) spectra, it appears that the reduced peak-intensities arise from reduced efficiency of cross polarization or interference of internal motions with proton decoupling frequencies. In particular, the E-F and F-G loops and some transmembrane helices of the bleached bO have acquired internal motions whose frequencies interfere with proton decoupling frequencies. In contrast, the protein backbone of the bO from the retinal-negative cells is incompletely folded. Although it contains mainly α-helices, its very broad ^{13}C NMR signals indicate that its tertiary structure is different from bR. Importantly, this changed structure is identical in form to that of bleached bO from wild-type bR after it was regenerated with retinal *in vitro*, and bleached with hydroxylamine. We conclude that the binding of retinal is essential for the correct folding of bR after it is inserted *in vitro* into the lipid bilayer, and the final folded state does not revert to the partially folded form upon removal of the retinal.

Key words: bacterio-opsin, bacteriorhodopsin, conformational change, membrane proteins, solid-state NMR.

Bacteriorhodopsin (bR) is an integral membrane protein, present as a trimer in the purple membrane of *Halobacterium salinarum*, which functions as a light-driven proton pump that translocates protons from the inside to the outside of the cell. Its three-dimensional structure at various resolutions has been elucidated by cryo-electron microscopy (*1–3*) and X-ray diffraction (*4–7*). Bacteriorhodopsin will spontaneously refold from a denatured state to a native state *in vitro* (*8–10*). For this reason, regeneration of bR from its bleached apoprotein, bacterio-opsin (bO), and retinal *in vitro* in natural or synthetic lipid bilayers has been utilized as a simple and convenient model system to study stability and folding behavior of polypeptide chains, as well as the oligomerization of integral membrane proteins (*8–12*). However, the completely correct folded state, *i.e.*, the same as that of native bR, was shown to be achieved only when the retinal was incorporated *in vivo* into bO from a chromophore-deficient strain, as judged from the establishment of the high pK_a of the Schiff base (*13*). Nevertheless, the photocycle of regenerated bR proved to be native-like, irrespective of *in vitro* or *in vivo* folding, probably because the structural perturbation imposed by photo-isomerization of the retinal may be sufficiently large to overcome any slight modification of side-chain orientation caused by *in vitro* folding in the vicinity of the Schiff base. It has also been demonstrated that fully active bR can be regenerated from enzymatically cleaved fragments (*14–16*), but insertion of an exogenous epitope into certain loops resulted in loss of function (*17*).

Kinetic studies showed that refolding of bR in lipid bilayers can be considered to involve at least two stages: (a) folding of the disordered form to α-helix, and (b) regeneration of bR upon noncovalent binding of retinal at its binding site, followed by formation of the Schiff base (*10*, *18–20*). It

[1] This work has been supported in part by Grants-in-Aid for Scientific Research (B) (09480179 and 09558094) and a Grant-in-Aid for International Scientific Research (Joint Research)M(10044092) from the Ministry of Education, Science, Sports and Culture of Japan.

[2] To whom corresponding should be addressed. Tel +81-791-58-0181, Fax: +81-791-58-0182, E-mail: saito@sci.himeji-tech.ac.jp

Abbreviations: bR, bacteriorhodopsin; bO, bacterio-opsin; CP-MAS, cross polarization-magic angle spinning; DD-MAS, dipolar decoupled-magic angle spinning.

is not clear, however, how the protein conformational changes are induced, or how the backbone dynamics is altered in such a system. These questions can be answered by systematic examination of the conformation-dependent displacements of ^{13}C NMR peaks and their amplitudes. In fact, we demonstrated distinct conformational changes of individual peptide chains in bO with and without retinal in ^{13}C NMR studies on [3-^{13}C] Ala-bR and -bO (*21*) that utilized conformation-dependent displacements of ^{13}C NMR shifts in various types of model systems as reference (*22–24*). The spectral changes of the protein backbone with and without retinal or retinal analogs proved to be useful means to study apoprotein–chromophore interactions (*21*). The ^{13}C NMR approach is of advantage for this purpose, because it probes backbone dynamics, which can cause selective suppression of certain peaks of CP-MAS NMR spectra due to the presence of either fast isotropic or large-amplitude motions with correlation time $<10^{-8}$ s, which arise through inefficient cross polarization from ^{1}H to ^{13}C (*25*), or intermediate isotropic or anisotropic motion in the order of 10^{-5} s, which prevents the narrowing of peaks through interference with proton decoupling both for CP-MAS and DD-MAS NMR spectra (*26*). This is evident if one compares the relative peak-intensities of ^{13}C CP-MAS NMR spectra of [3-^{13}C] Ala bR and -bO with those of DD-MAS NMR spectra. These labels probe the *backbone* dynamics in spite of the location of ^{13}C label on the side-chain, as long as the time scale of the motion is different from the methyl rotation, which is faster than 10^{8} Hz. Indeed, the probe of [3-^{13}C]Ala-bO or bR was very sensitive to conformation and dynamics of protein backbones (*22–24*).

In the present paper, we aimed to clarify at what stage of the folding of bR the correct conformational changes are induced, by means of a ^{13}C NMR study on [3-^{13}C]Ala- and [1-^{13}C]Val-bO, either isolated from a retinal-deficient strain or obtained by bleaching bR. The approach using the former label was made possible by the recent improvement in spectral resolution that identifies up to 12 peaks together with newly assigned ^{13}C NMR peaks to Ala residues in individual positions (*27–29*). Surprisingly, we found that bO from the retinal-deficient strain gave rise to very broad ^{13}C NMR signals, although most of the individual peak-positions are characteristic of α_{II}–helix conformations undergoing local anisotropic conformational fluctuations. This spectral pattern changed to show well-resolved signals characteristic of bleached bO, once retinal was incorporated *in vitro* and then removed. This means that retinal is essential for the unique folding that leads to bR. The structure of this state is retained even after the retinal is removed by bleaching.

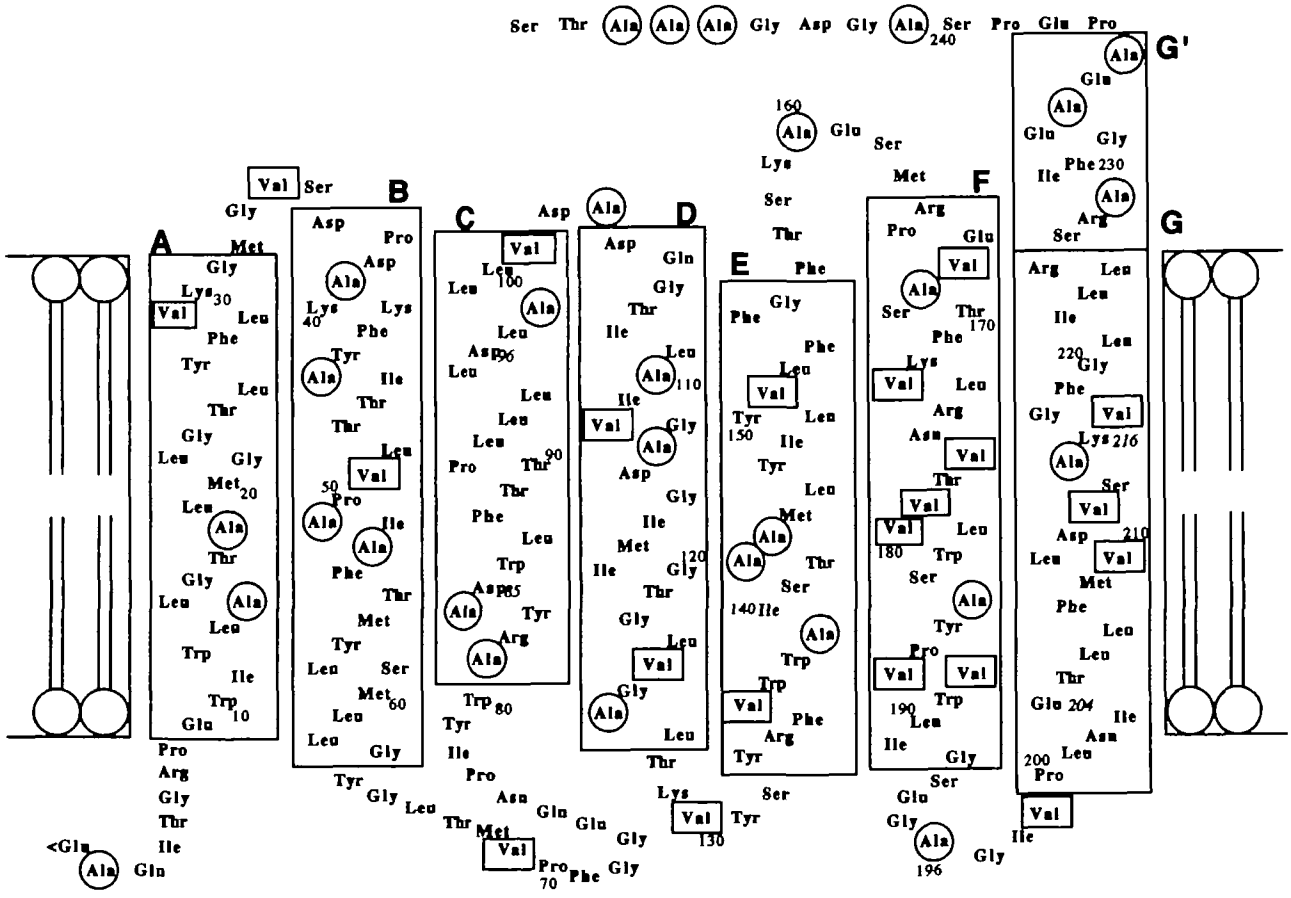

Fig. 1. **A schematic representation of the secondary structure of bR based on recent X-ray diffraction study (7).** The transmembrane helices A–G and the α-helical segments protruding from the membrane surface G′ (*34*) are shown by columns. The circled and boxed residues are ascribed to Ala and Val residues, respectively

MATERIALS AND METHODS

Sample Preparation—L-[3-^{13}C]Alanine and [1-^{13}C]valine were purchased from CIL, Andover, MA, USA, and used without purification. *H. salinarum* S9 and A84G, A39V, and E1001 (wild type but ret$^-$) mutants were grown in the TS medium described by Onishi *et al.* (*30*), in which unlabeled L-alanine or valine was replaced by either [3-^{13}C]Ala (circled) or [1-^{13}C]Val residues (boxed) as shown in a schematic representation of the secondary structure of bR based on recent X-ray diffraction (*7*) (see Fig. 1). It turned out that no isotope scrambling from [3-^{13}C] alanine to other amino acid residues occurred, except for conversion to the lipid peaks at 19.8, 22.7, 37.6, and 39.5 ppm as demonstrated by our previous ^{13}C NMR study on denatured [3-^{13}C] Ala-bR solubilized in [^2H]trifluoroacetic acid (*31*). Purple membranes were then isolated by a standard method (*32*). To prepare bO from bR, hydroxylamine solution (0.5 M, pH 7) was added to the purple membrane, which was then exposed to panchromatic light for 20 h at 23°C (*33*). The bO preparation thus obtained was washed with bovine serum albumin 8 times and suspended in 5 mM HEPES buffer containing 0.02% NaN_3 and 10 mM NaCl at pH 7. The samples were concentrated by centrifugation, and pelleted preparations thus obtained were contained in a 5 mm o.d. zirconia pencil-type rotor. Teflon caps were tightly glued to the rotor to prevent dehydration through a pinhole in caps during magic angle spinning under a stream of dried compressed air.

Measurements of ^{13}C NMR—100.6 MHz high-resolution ^{13}C NMR spectra were recorded in the dark at 20°C on a Chemagnetics CMX-400 NMR spectrometer, both by CP-MAS and DD-MAS methods, to distinguish the time scale of conformational fluctuation mentioned above, if any. The spectral width and contact, repetition, and acquisition times for CP-MAS NMR experiments were 40 kHz, 1 ms, 4 s, and 50 ms, respectively. The $\pi/2$ pulses for carbon and proton nuclei were 5 μs, and the spinning rate was 2.6 and 4 kHz for [3-^{13}C]Ala- and [1-^{13}C]Val-labeled proteins, respectively. Free induction decays were acquired with data points of 2 K. Fourier transform was carried out as 16 K points after 14 K points were zero-filled. ^{13}C chemical shifts were referred to the chemical shifts of the carboxyl signal of glycine [176.03 ppm from tetramethylsilane (TMS)] and converted to the relative shifts from TMS.

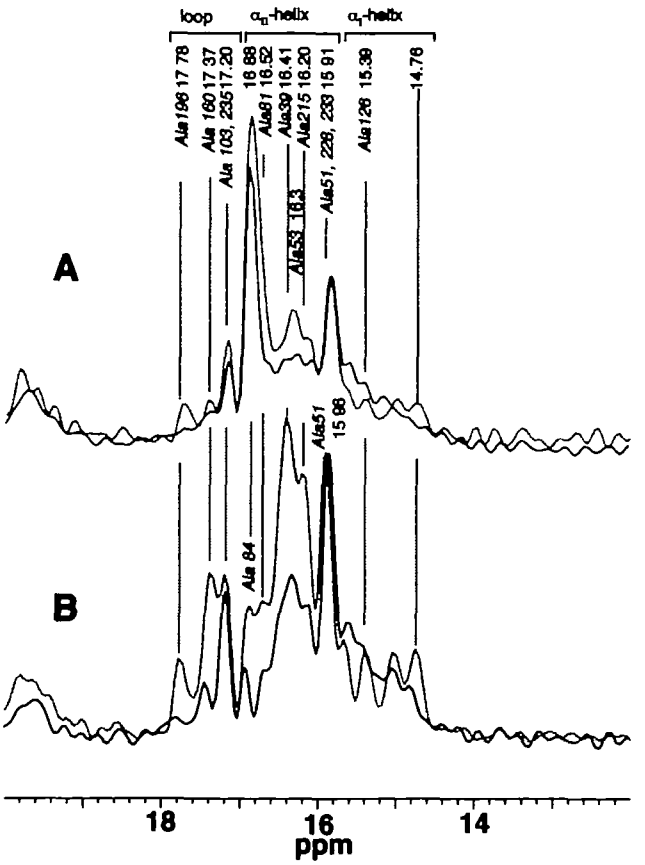

Fig. 2. **^{13}C NMR spectra of [3-^{13}C]Ala-labeled bacterio-opsin (bO) (black traces) and bacteriorhodopsin (bR) (gray traces) recorded by DD-MAS (A) and CP-MAS (B).** Numbers of transients for DD-MAS experiments are 11,132 and 5,100 for bR and bO, respectively. Numbers of transients for CP-MAS experiments are: 8,000 and 9,580 for bR and bO, respectively Intensity standard for the spectral comparison was taken from the peak at 15 91 ppm ascribed to the α-helical segments protruding from the membrane surface. Regio-specific assignment of peaks are illustrated above the traces.

RESULTS

Figure 2, A and B, compares the expanded 100.6 MHz ^{13}C NMR spectra of [3-^{13}C]Ala-labeled bO prepared by bleaching bR (black traces) and bR (gray traces) (12–20 ppm from TMS) as recorded by DD-MAS (A) and CP-MAS (B) methods at ambient temperature (20°C), respectively. No other signal from the natural abundance ^{13}C pertaining from other residues overlapped this region, as mentioned previously (*31*). The regio-specific assignment of peaks to the loop and transmembrane α_I- and α_{II}-helices for bR are illustrated above the traces. The intensity standard for the spectral comparison between bR and bO was taken from the peak-intensities at 15.91 ppm, which seemed to be less sensitive to the presence or absence of retinal because of its

TABLE I **^{13}C chemical shifts of [3-^{13}C]Ala-, [1-^{13}C]Ala-, and [1-^{13}C]Val-labeled bacteriorhodopsin at 20°C (ppm).**

	Location	CH_3	C=O	Methods	References
Ala 39	Helix B	16 40		A39V	This work
51	Helix B	15 96		A51G, Mn^{2+} binding	*29*
53	Helix B	16.3	177.9	A53G, A53V	*34, 35*
81	Helix C	16.52		A81G, Mn^{2+} binding	*29*
84	Helix C	16.88		A84G	This work
103	C-D Loop	17 20*		A103C	This work
126	Helix D	15 39		A126G	*27*
160	E-F Loop	17 38*		A160G	*37*
196	F-G Loop	17 78		A196G	*27*
215	Helix G	16 20		A215G Mn^{2+}	*29*
228, 233	Helix G′	15.91		Limited proteolysis	*34*
240, 244–246	C-terminal	16.88		Limited proteolysis	*34*
Val 49	Helix B		172.0	V49A	*36*
69	B-C Loop		173.0	Limited proteolysis	*36*
199	F-G Loop		171.1	V199A	*36*

*These peaks are displaced depending upon temperature.

location at the α-helical portion, which protruded mainly from the membrane surface (*34*). This assumption was justified in view of the presence of at least two unchanged intensities at 17.20 and 15.39 ppm. As pointed out previously (*21*, *34*), an alternative comparison of spectra between the DD-MAS and CP-MAS experiments showed that some peak-intensities of the former at 16.88 and 15.91 ppm from the C-terminal residues substantially decreased relative to the latter, because of insufficient efficiency of cross polarization due to the presence of isotropic motions for the terminal end of the C-terminus anchored at the membrane surface with correlation time $<10^{-8}$ s. This view was confirmed by examination of ^{13}C NMR spectra of enzymatically cleaved bRs (*34*, *35*). This is true for further spectral comparison of bO between the DD-MAS and CP-MAS experiments, as shown in Fig. 2.

Under the improved spectral resolution, twelve peaks have been resolved for bO, in contrast to the previous observation of only five resolved peaks (*21*). The same lineshape as in the previous report can be reproduced from the current experimental data, however, by ignoring the latter half of the data points of the currently observed free induction decays. Naturally, the positions of the intense peaks are in good agreement with the previous data of low resolution (*21*, *34*), although some less intense peaks, for instance, 17.78, 17.37, 16.72 ppm, were not resolved previously, as pointed out already in the case of bR. Further, this may happen when extensive peak-enhancement for bO spectra (Gaussian broadening of 50 Hz in this case *vs.* 25–30 Hz in the usual case) is applied.

The assignment of the ^{13}C NMR signals for bR, based on comparison of ^{13}C NMR spectra of the wild type with those of site-directed mutants, Mn^{2+} binding, and enzymatic cleavages (Table I), should be directly applicable to bO provided that the peak-positions for bO are not significantly changed from those of bR. It is, therefore, noted that the lowermost peak of Ala C_β signals at 17.78 ppm, ascribed to Ala 196 also in bO, is suppressed in both DD-MAS and CP-MAS NMR spectra. This is due to the presence of either isotropic or anisotropic motions with time scale of 10^{-5} s in the F-G loop which interfere with proton decoupling frequencies (~50 kHz) (*26*). Still, substantial suppression of the relative intensities at the peaks from 16.88 to 16.19 ppm (the transmembrane α-helices) in both the CP-MAS and DD-MAS spectra cannot be ignored, mainly due to interference of the intermediate backbone motions with time scale of 10^{-5} s with proton decoupling frequencies mentioned above (*26*).

To help assign such suppressed peaks to specific amino acid residues, we have recorded the ^{13}C CP-MAS NMR spectra of A84G (Fig. 3A) and A39V mutants (Fig. 3B) and

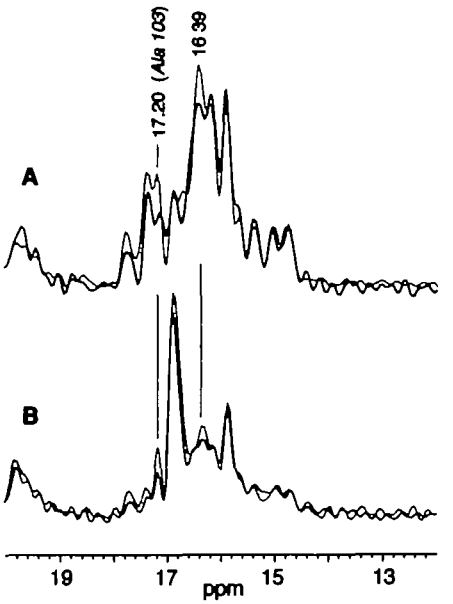

Fig. 4 ^{13}C CP-MAS NMR (A) (5,000 transients) and DD-MAS (B) (5,080 transients) spectra of [1-^{13}C]Ala-labeled A103C (black traces) as compared with those of wild type (gray traces).

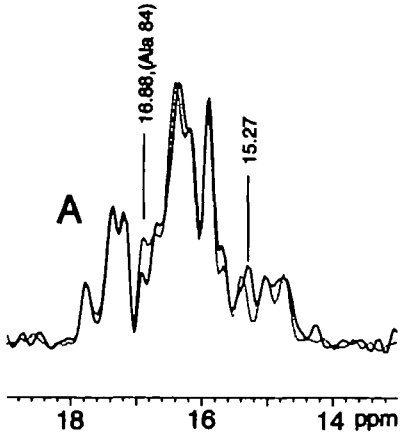

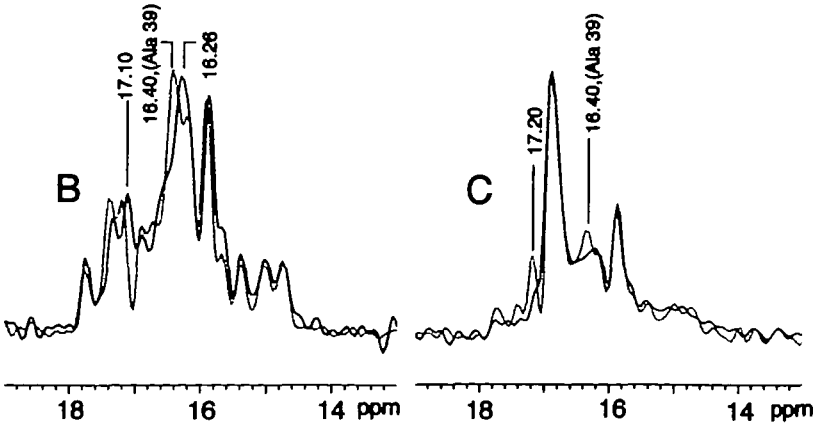

Fig. 3 ^{13}C CP-MAS NMR spectra of [3-^{13}C] Ala-labeled A84G (A) (8,880 transients) and A39V mutants (B) (10,100 transients) and DD-MAS NMR spectrum of A39V (C) (black traces) as compared with those of wild type (gray traces). The intensity standard is from the peak at 15.81 ppm. The assigned peak based on the experiment here is shown by the arrowed peak.

the DD-MAS NMR spectrum of the latter (Fig. 3C) (black traces) as compared with those of the wild type (gray traces). The peak at 15.91 ppm was again taken as intensity standard for the spectral comparison. It is straightforward to assign the peak at 16.88 ppm to Ala 84, as it is decreased in A84G relative to the wild type, although an additional peak from Ala 240 from the C-terminal moiety is superimposed upon it. In a similar manner, the most intense peak at 16.40 ppm of A39V in the DD-MAS NMR spectrum free from efficiency of cross polarization (Fig. 3C) was clearly decreased as compared with the wild type, although several other places were also modified, as seen by the increased peak-intensity at 16.26 ppm in the CP-MAS NMR spectrum (Fig. 3B) as well as the upfield displacement of the peak (Ala 103, to be assigned below) at 17.20 to 17. 10 ppm at the loop region. This is because Ala 39 is located at turn of the helix B at its cytoplasimc end (see Fig. 1), and its replacement with Val may result in accompanied modification of the secondary structure of helix B at the cytoplasmic end and C-D loop through interactions among cytoplasmic loops and C-terminal α-helix (*29*). Concomitantly, the decreased peak at 17.20 ppm of A103C in Fig. 4 is unequivocally assigned to Ala 103, which overlaps the Ala 235 peak of the C-terminus, although the Ala 39 peak is also affected by the above-mentioned modification of the secondary structure of helix B at the cytoplasmic end and C-D loop. The peak at 17.37 ppm is therefore assigned to Ala 160, although ^{13}C NMR spectra of Ala 160G or A160V were severely modified (spectra not shown).

As illustrated in Fig. 5, we compare the ^{13}C NMR spectrum of [1-^{13}C]Val-labeled bO produced by bleaching with that of bR. The three previously assigned Val signals are indicated on the individual peaks that resonate at the higher field region (*36*), because they are ascribed to Val residues followed by a Pro residue, namely, Val 199 and Val 69 at the F-G and B-C loops, respectively, and Val 49 at the B helix, which are displaced upfield by *ca.* 2 ppm by the "proline" effect (*37*, *38*), although they are superimposed upon another peak, as discussed in our previous paper (*36*). The intensities of these three peaks of bO were significantly decreased when retinal was removed by bleaching, because the fortuitously superimposed peaks in bR are resolved into separate peaks in bO, due to an accompanying conformational change, which are located at least at the B-C (Val 69) and F-G (Val 199) loops; and they are also partly suppressed by acquired internal motions that interfere with magic angle spinning as in the situation of [3-^{13}C]Ala-bR mentioned above. As to the former possibility, Val 199 and 49 are displaced upfield and downfield by 0.2 and 0.4 ppm upon conversion of bR to bO, respectively, although they are coupled with the intensity change of Ala 196 in the same F-G loop as Val 199 of [3-^{13}C] Ala-bO and also the peak-suppression at the α_{II}-helices at 16.17–16.88 ppm. As to the latter possibility, the peak-intensities of the peaks resonated at 174.6 ppm, and the three peaks of Val 199, 49, and 69 seemed to be suppressed to some extent, although they are not completely suppressed as in the case of [1-^{13}C] or [2-^{13}C] Ala-bR (*29*).

On the basis of these arguments, we concluded that the secondary structure of bleached bO is more flexible than

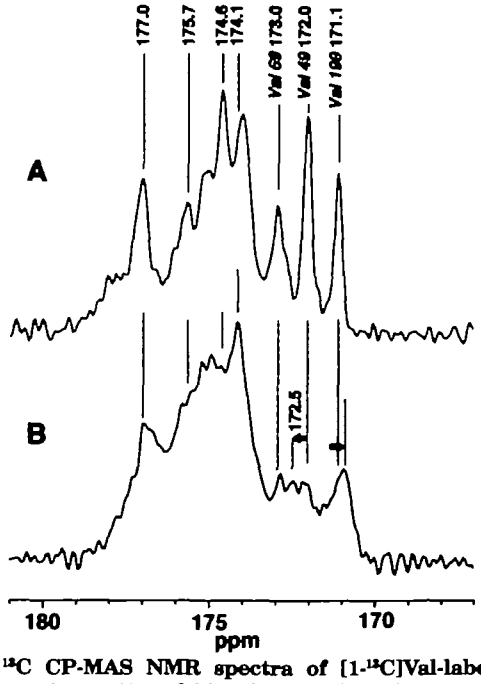

Fig 5. **^{13}C CP-MAS NMR spectra of [1-^{13}C]Val-labeled bR (8,000 transients; A) and bleached bO from bR (10,524 transients; B).** The displaced peaks by removal of retinal are shown by the arrows.

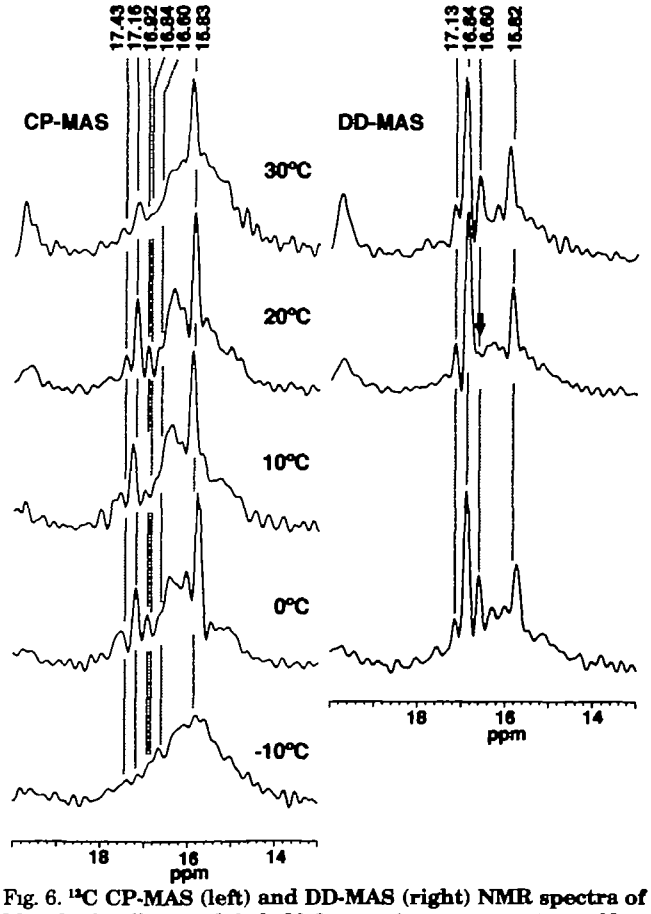

Fig. 6. **^{13}C CP-MAS (left) and DD-MAS (right) NMR spectra of bleached [3-^{13}C] Ala-labeled bO at various temperatures.** Note that the arrowed peak at 20°C disappears at 20°C but appears at higher or lower temperatures.

that of bR. To clarify this point further, we examined the thermal stability of the secondary structure of bO, relative to that of bR, by recording the ^{13}C NMR spectra of bO (Fig. 6) and bR (Fig. 7) at various temperatures between −10 and 40°C (*30*). It is interesting that the peak labeled with the arrow at 16.60 ppm in the DD-MAS NMR spectra (Fig. 6) is suppressed at 20°C but clearly visible at both 30 and 0°C, although this signal is not significantly changed in this temperature range in the CP-MAS NMR spectra. This is probably, a case in which large-amplitude, isotropic motion, resulting in reduced efficiency of the cross polarization, with correlation time $<10^{-6}$ s, is present at certain transmembrane helices at the cytoplasmic surface at 30°C, but this motion is slowed down to the time scale of 10^{-5} s at 20°C. Interestingly, the well-resolved signals of bO at 17.43 (Ala 160) and 17.16 ppm (Ala 103) from the loops and 15.83 ppm from the C-terminal α helix (*21, 34*) at temperature between 0 and 20°C are almost completely suppressed at −10°C and are changed to the spectral pattern of bO purified from the retinal-deficient mutant E1001 at ambient temperature (Fig. 8). It is worth mentioning that the peak from the C-terminus helix (15.92 ppm at 30°C–15.77 ppm at 0°C) disappeared at −10°C in both CP-MAS and DD-MAS spectra due to interference of molecular motion with proton decoupling frequency (*26*).

In contrast, no peak of bR exhibits a significant intensity change with temperature like the 16.60 ppm in DD-MAS NMR peak of bO. A relative intensity change of 16.19 *vs.* 16.41 ppm in the CP-MAS spectra at elevated temperature above 30°C was noted, and the peaks from the loop regions also varied with temperature (see Fig. 7). Ala 39 (16.40 ppm) may be responsible for such temperature-dependent signals, in view of its location at the cytoplasmic turn of the B helix. Consistent with our previous findings (*34*), the α-helical peak of the C-terminus from 15.91 ppm is displaced upfield to the position of bO at 15.70 ppm at a temperature between 20 and 10°C and finally suppressed below 10°C, as a result of interference with proton decoupling frequencies (*26*). It is noteworthy that this sort of spectral change is related with accompanying changes of Ala 160 and 103 in the loop regions (Fig. 7).

Figure 8 illustrates the ^{13}C DD-MAS (top) and CP-MAS (bottom) NMR spectra of [3-^{13}C]Ala-labeled bO from the retinal-deficient strain E1001. It is noteworthy that the linewidths of the observed spectra of native bO from E1001 strain are not the same as those from [3-^{13}C]Ala-bO prepared by bleaching of bR, shown in Fig. 2, except for the presence of the three intense narrow peaks, distinct in the DD-MAS but absent in the CP-MAS spectra. The ^{13}C NMR signals of the transmembrane α-helices in this case are substantially broadened as compared with those of the bleached bO (Fig. 2A). Obviously, these two signals at 15.84 and 16.86 ppm arose from the C-terminal residues, which undergo isotropic or large-amplitude motions with correlation time less than 10^{-8} s, resulting in reduced efficiency of cross polarization in the case of the *in vivo* produced bO preparation (*21, 34*). The major secondary structure of the individual chains from the transmembrane portion arises from the α-helix conformation on the basis of their peak-positions (*22–24*), and the peaks from the loop region for three Ala residues seem to be significantly suppressed because of inherent molecular motions.

Figure 9A illustrates the ^{13}C CP-MAS NMR spectrum of regenerated bR prepared by addition of retinal to the [3-^{13}C]Ala-labeled bO from E1001 strain *in vitro* at ambient temperature. In accordance with our previous work on such

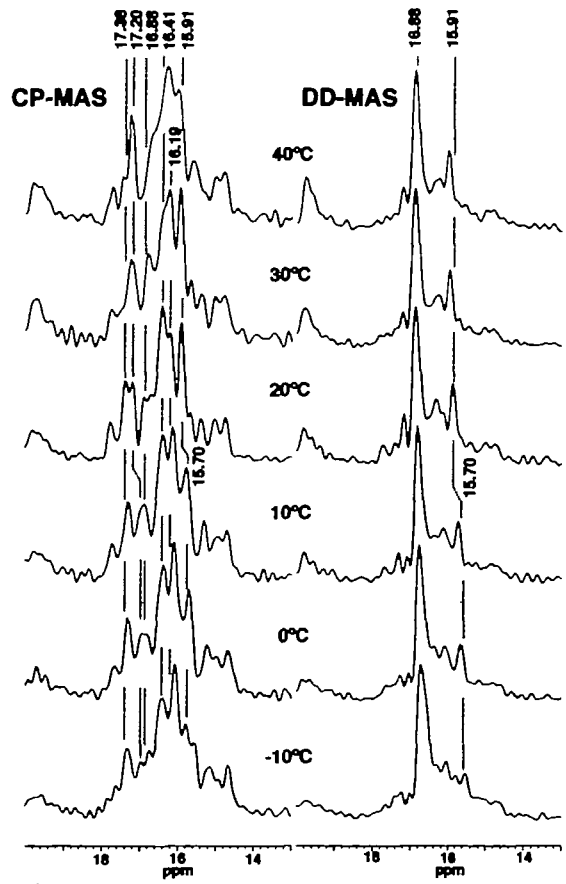

Fig. 7. **^{13}C CP-MAS (left) and DD-MAS (right) NMR spectra of bleached [3-^{13}C] Ala-labeled bR at various temperatures as reference.**

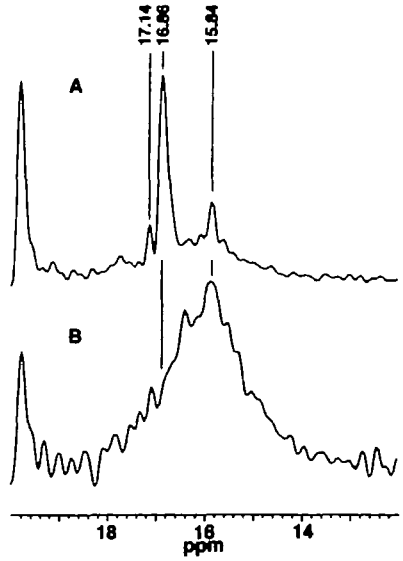

Fig. 8 **^{13}C DD-MAS (10,100 transients; A) and CP-MAS (8,800 transients; B) NMR spectra of [3-^{13}C] Ala-labeled bO from retinal-deficient E1001 mutant.**

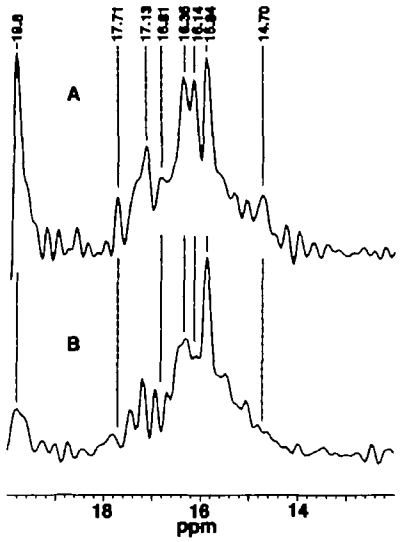

Fig. 9. **^{13}C CP-MAS NMR spectra of regenerated [3-^{13}C] Ala-labeled bR prepared by addition of retinal to retinal-deficient mutant *in vitro* (A) and bleached bO resulting from removal of retinal from the regenerated bR (B).**

regenerated bR (*21*), the characteristic ^{13}C NMR spectral pattern of bR was observed. It turned out that bleached bO prepared from this regenerated bR gave rise to a ^{13}C NMR spectral pattern (Fig. 9B) identical to that of bleached bO prepared from *in vivo* folded bR (Fig. 2B). In the preparation in Fig. 9B, the above-mentioned peaks from the C-terminus at 15.84 and 17.13 ppm reappeared which are responsible for the moiety undergoing intermediate motions detected by the prolonged proton spin-lattice relaxation times in the rotating frame (*21*). This kind of motional feature was not detected in bR. It probably arises from the C-terminal helix (designated as G′ helix; see Fig. 1), which is attached to helix G undergoing conformational fluctuations as judged from the motions detected at the F-G loop because of modified interactions with cytoplasmic loops.

DISCUSSION

Role of Retinal as a Template for Irreversible Secondary Folding of bR—As illustrated in Figs. 2 and 8, we found that the secondary structures of the two types of bO preparations consist of mainly α-helix conformations (*22–24*), consistent with the previous findings (*8*, *10*). Nevertheless, it is obvious that the ^{13}C NMR spectral patterns of these two preparations are different from each other: the bleached preparation gave rise to well-resolved peaks, while bO from the retinal-deficient strain gave very broad signals. In particular, the characteristic peaks ascribable to the loop regions are obscured in the latter, probably because these peaks are suppressed by the intermediate motions which interfere with proton decoupling frequencies of the order of 10^5 Hz (*26*). Kinetic studies on bR regeneration utilizing CD or fluorescence spectroscopy showed a folding model consisting of at least two intermediate steps, formation of a partially folded apoprotein intermediate (I_o), and non-covalent binding of retinal (I_R) with a time scale of milliseconds to seconds (*10*, *19*). More recently, two additional intermediates have been included (*20*, *39*). Nevertheless, because of lack of specific means to probe conformational changes by spectroscopic methods, it is not clear how the conformation of the protein backbone is altered by formation of a Schiff base. It is likely that the α-helix form of bO from the retinal-deficient strain represents a partially folded apoprotein (see Fig. 8), which is not necessarily an assembly of unique structures but an aggregate undergoing slow chemical exchange among various slightly different conformers with a time scale of milliseconds. The very greatly broadened spectral feature implies such a time scale of chemical exchange (*40*).

It appears, however, that once the correctly folded structure is attained, the secondary structure of bO is retained even after the retinal is removed, because the conformational change associated with bleaching and regeneration is completely reversible between the native and bleached preparations. In contrast, as demonstrated in Figs. 2, 8, and 9, a drastic spectral change of bO from the retinal-deficient strain was noted from its broad featureless signals (Fig. 8B), different from the well-resolved ^{13}C NMR spectra (Fig. 9B) characteristic of bleached bO (see Fig. 3B) prepared from regenerated bR (see Fig. 9A). This means that an irreversible conformational change was induced in the final step of Schiff base formation, perhaps leading by oligomerization to the trimeric form, although confirmation of lattice structure by circular dichroism (*41*, *42*) is not feasible. The trimeric form is stabilized by hydrophobic packing of the helix–helix interaction between helix B and helix D of neighboring bR molecules (*5*, *43*, *44*), although the present observation shows that helix B, as viewed from suppressed peaks of Ala 39 and 53, is involved in conformational fluctuation in the order of 10^{-5} s, as will be discussed below. It is therefore understandable that the flexibility of protein backbone is mainly determined by the presence or absence of this sort of helix–helix interaction modulated by the presence or absence of a Schiff base in bR or bO, respectively. In this connection, the very broad ^{13}C NMR peaks for bleached bO at −10°C (Fig. 6), which was ascribed to the presence of peptide chains of irregularly frozen (*40*), is realized for bO from retinal-deficient strain even at ambient temperature, if such trimeric form is not present without correct folding.

Conformational Changes of Protein Backbone and Changed Dynamics, Due to Formation of bO from bR—The conformation and the dynamics of the protein backbone are altered at several sites upon conversion of bR to bO by removal of retinal. In particular, the relative peak-intensities of the transmembrane α_{II}-helices of bO, which resonate between 16.17 and 16.88 ppm, were significantly suppressed as compared with those of bR, both in the CP-MAS and DD-MAS NMR spectra. This kind of intensity change was not discussed before (*21*) because digital spectral resolution was insufficient. The suppression of peaks in both the CP-MAS and DD-MAS NMR spectra can be ascribed to motions that interfered with proton decoupling frequencies, in the order of time scale of 10^{-5} s. Very similar spectral changes at this spectral region are found in the ^{13}C NMR spectra of M-like state of D85N mutant at pH 10, in which global conformational changes were induced when constraints to the protein backbone from the retinal were temporally relaxed due to deprotonation of the Schiff base (Kawase *et al.*, manuscript in preparation) (*45*, *46*). In the 3D structure observed by cryo-electron microscopy (*1–3*) or

X-ray diffraction (*4–7*), Ala 215 (helix G), Ala 53, and Val 49 (helix B), which are located at positions very close to the Schiff base, are among the residues at which the local conformation may be most affected. These signals were originally at 16.20 ppm (Ala 215), 16.4 ppm (Ala 53), and 172.0 ppm (Val 49), as summarized in Table I. Therefore, part of the suppressed peaks at 16.41 and 16.19 ppm could be ascribed to these residues which are displaced upfield or suppressed due to acquired motional freedom of the order of 10^{-5} s. Further, one of the resolved peaks, from Val 49 (helix B), that originally resonated at 172.0 ppm was displaced downfield to around 172.5 ppm, when the helix–helix interaction was absent after removal of retinal, as encountered also for a single synthetic [1-^{13}C] Val^{49}-labeled fragment B (*36–71*) of bR incorporated into DMPC bilayer (*48*). In a similar manner, Ala 84 (helix C) signal at 16.88 ppm and Ala 39 (helix B) at 16.40 ppm (Fig. 3) might be also affected by such relaxed interaction between the Schiff base and Asp 85. At present, it is not certain to which Ala residue the highermost peak at 14.76 ppm is ascribed. Undoubtedly, this signal could be an Ala residue located where the retinal polyene is sandwiched between Trp 86 and Trp 182, or the β-ionone ring of retinal is flanked by Trp 138 and 189, because its peak-intensity was suppressed in bO. One possibility is Ala 139, which is close to Trp 138. Assignment of this peak based on site-directed mutagenesis is under way.

Spectral changes were also noteworthy in the signals from the loop region: Ala 196 signal (F-G loop) at 17.78 ppm and Ala 160 signals (E-F loop) at 17.37 ppm of bO are substantially decreased both in the CP-MAS and DD-MAS NMR spectra. Undoubtedly, these kinds of the spectral changes could also be ascribed to intermediate motions that interfere with proton decoupling frequencies on the time scale of 10^{-5} s (*26*), in addition to the presence of slow local fluctuation of amide unit responsible for the presence of α_{II} helix (~10^{-2} s) (*47*). So far, we have pointed out that ^{13}C NMR signals of Ala 39, 53, 84, and 215, and Val 49 in the transmembrane helices and Ala 196 and Val 199 in the F-G loop might be influenced by the induced intermediate motions in bO. It is conceivable that the presence of this sort of conformational flexibility facilitates incorporation of retinal to form bR. In fact, on the basis of molecular dynamics simulations (*48*), Schulten and coworkers pointed out that the binding pathway of retinal to bO is through a window between bR helices E and F.

Concluding Remarks—We have demonstrated that irreversible or reversible conformational changes are induced in the regeneration of bR from bO, either from the retinal-deficient strain or bleaching of bR, respectively. In particular, we showed that an irreversible conformational change of the protein backbone was induced when retinal was incorporated into bO from the retinal-deficient strain. It is probable that the tertiary structure of bO is retained even after retinal is removed, because the subsequent conformational change is reversible. Further, the secondary structures of bO and bR can be simply characterized as flexible or inflexible backbone dynamics with or without slow motions of μs order for bO and bR, respectively, both in the transmembrane and loop regions, as a result of covalent binding of retinal to form a Schiff base. This sort of flexibility in the former may be essential for entry of retinal into bO.

REFERENCES

1. Henderson, R., Baldwin, J.M., Ceska, T.A., Zemlin, F., Beckman, E., and Downing, K.H. (1990) Model for the structure of bacteriorhodopsin based on high-resolution electron cryo-microscopy *J. Mol. Biol* **213**, 899–929
2. Grigorieff, N., Ceska, T.A., Downing, K.H., Baldwin, J.M., and Henderson, R. (1996) Electron-crystallographic refinement of the structure of bacteriorhodopsin. *J. Mol. Biol* **259**, 393–421
3. Kimura, Y., Vassylyev, D.G., Miyazawa, A., Kidera, A., Matsushima, K., Mitsuoka, K., Murata, K., Hirai, T., and Fujiyoshi, Y. (1997) Surface of bacteriorhodopsin revealed by high-resolution electron crystallography. *Nature* **389**, 206–211
4. Pebay-Peyroula, E., Rummel, G., Rosenbusch, J.P., and Landau, E.M. (1997) X-ray structure of bacteriorhodopsin at 2.5 angstroms from microcrystals grown in lipidic cubic phases. *Science* **277**, 1676–1681
5. Essen, L., Siegert, R., Lehmann, W.D., and Oesterhelt, D. (1998) Lipid patches in membrane protein oligomers: crystal structure of the bacteriorhodopsin-lipid complex. *Proc. Natl. Acad. Sci. USA* **95**, 11673–11678
6. Luecke, H., Richter, H.T., and Lanyi, J.K. (1998) Proton transfer pathways in bacteriorhodopsin at 2.3 angstrom resolution. *Science* **280**, 1934–1937
7. Luecke, H., Schobert, B., Richter, H-T., Cartailler, J-P. and Lanyi, J.K. (1999) Structure of bacteriorhodopsin at 1.55 Å resolution. *J Mol. Biol* **291**, 899–911
8. Huang, K-S., Bayley, H., Liao, M-J., London, E. and Khorana, H.G. (1981) Refolding of an integral membrane protein. Denaturation, renaturation and reconstitution of intact bacteriorhodopsin and two proteolytic fragments. *J Biol. Chem.* **256**, 3802–3809
9. London, E. and Khorana, H.G. (1982) Denaturation and renaturation of bacteriorhodopsin in detergents and lipid-detergent mixtures. *J. Biol. Chem.* **257**, 7003–7011
10. Booth, P.J., Flitsch, S.L., Stern, L.J., Greenhalgh, D.A., Kim, P.S., and Khorana, H.G. (1995) Intermediates in the folding of the membrane protein bacteriorhodopsin *Nat. Struct. Biol.* **2**, 139–143
11. Braiman, M.S., Stern, L.J., Chao, B.H., and Khorana, H.G. (1987) Structure-function studies on bacteriorhodopsin IV. Purification and renaturation of bacterio-opsin polypeptide expressed in *Escherichia coli*. *J Biol Chem.* **262**, 9271–9276
12. Marti, T. (1998) Refolding of bacteriorhodopsin from expressed polypeptide fragments. *J. Biol. Chem.* **273**, 9312–9322
13. Kollbach, G., Steinmuller, S., Berndsen, T., Buss, V., and Gartner, W. (1998) The chromophore induces a correct folding of the polypeptide chain of bacteriorhodopsin. *Biochemistry* **37**, 8227–8232
14. Trewhella, J., Popot, J-L., Zaccai, G., and Engelman, D.M. (1986) Localization of two chymotryptic fragments in the structure of renatured bacteriorhodopsin by neutron diffraction. *EMBO J.* **5**, 3045–3049
15. Kahn, T.W., Sturtevant, J.M., and Engelman, D.M. (1992) Thermodynamic measurements of the contributions of helix-connecting loops and of retinal to the stability of bacteriorhodopsin. *Biochemistry* **31**, 8829–8839
16. Kahn, T.W. and Engelman, D.M. (1992) Bacteriorhodopsin can be refolded from two independently stable transmembrane helices and the complementary five-helix fragment. *Biochemistry* **31**, 6144–6151
17. Teufel, M., Pompejus, M., Humbel, B., Friedrich, K., and Fritz, H.J. (1993) Properties of bacteriorhodopsin derivatives constructed by insertion of an exogenous epitope into extra-membrane. *EMBO J.* **12**, 3399–3408
18. Popot, J.L., Gerchman, S.E., and Engelman, D.M. (1987) Refolding of bacteriorhodopsin in lipid bilayers. A thermodynamically controlled two-stage process. *J. Mol. Biol.* **198**, 655–676
19. Popot, J.L. and Engelman, D.M. (1990) Membrane protein folding and oligomerization: the two-stage model. *Biochemistry* **29**, 4031–4037

20. Booth, PJ , Farooq, A., and Flitsch, S.L (1996) Retinal binding during folding and assembly of the membrane protein bacteriorhodopsin. *Biochemistry* **35**, 5902–5909
21. Tuzi, S., Yamaguchi, S., Naito, A., Needleman, R., Lanyi, J.K., and Saitô, H (1996) Conformation and dynamics of [3-^{13}C]Ala-labeled bacteriorhodopsin and bacteriooopsin, induced by interaction with retinal and its analogs, as studied by ^{13}C nuclear magnetic resonance. *Biochemistry* **35**, 7520–7527
22. Saitô, H (1986) Conformation-dependent ^{13}C chemical shifts a new means of conformational characterization as obtained by high-resolution solid-state NMR. *Magn. Reson. Chem* **24**, 835–852
23 Saitô, H. and Ando, I (1989) High-resolution solid-state NMR studies of synthetic and biological macromolecules. *Annu. Rep. NMR Spectrosc.* **21**, 209–290
24 Saitô, H , Tuzi, S , and Naito, A. (1998) Empirical *versus* non-empirical evaluation of secondary structure of fibrous and membrane protein by solid-state NMR: a practical approach. *Annu Rep. NMR Spectrosc.* **36**, 79–121
25 Mehring, M (1983) *Principle of High Resolution NMR in Solids*, 2nd ed , Springer Verlag, New York
26 Rothwell, W P and Waugh, J.S (1981) Transverse relaxation of dipolar coupled spin system under rf irradiation:detecting motions in solid. *J. Chem. Phys.* **74**, 2721–2732
27 Tuzi, S , Yamaguchi, S , Tanio, M., Konishi, H., Inoue, S , Naito, A., Needleman, R., Lanyi, J K., and Saitô, H. (1999) Location of a cation-binding site in the loop between helices F and G of bacteriorhodopsin as studied by ^{13}C NMR. *Biophys. J.* **76**, 1523–1531
28. Tanio, M , Tuzi, S , Yamaguchi, S., Kawaminami, R., Naito, A., Needleman, R., Lanyi, J.K., and Saitô, H. (1999) Conformational changes of bacteriorhodopsin along the proton-conduction chain as studied with ^{13}C NMR of [3-^{13}C]Ala-labeled protein:Arg82 may function as an information mediator. *Biophys. J.* **77**, 1577–1584
29. Yamaguchi, S. (2000) Folding and surface dynamics of bacteriorhodopsin as studied by ^{13}C NMR. Ph D Thesis, Himeji Institute of Technology.
30. Onishi, H , McCance, E., and Gibbons, N E (1965) A synthetic medium for extremely halophilic bacteria *Can J. Microbiol.* **11**, 365–373
31. Tuzi, S , Naito, A., and Saitô, H. (1993) A high-resolution solid-state ^{13}C-NMR study on [1-^{13}C]Ala and [3-^{13}C]Ala and [1-^{13}C]-Leu and Val-labelled bacteriorhodopsin Conformation and dynamics of transmembrane helices, loops and termini, and hydration-induced conformational change *Eur. J .Biochem* **218**, 837–844
32 Oesterhelt, D and Stoeckenius, W. (1974) Isolation of the cell membrane of *Halobacterium halobium* and its fractionation into red and purple membrane. *Methods Enzymol* **31**, 667–678
33. Ebrey, T.G. (1982) *Methods Enzymol* **88**, 516–521
34. Yamaguchi, S., Tuzi, S., Seki, T , Tanio, M., Needleman, R., Lanyi, J.K., Naito, A. and Saitô, H (1998) Stability of the C-terminal alpha-helical domain of bacteriorhodopsin that protrudes from the membrane surface, as studied by high-resolution solid-state ^{13}C NMR *J Biochem.* **123**, 78–86
35 Tuzi, S , Naito, A., and Saitô, H. (1994) ^{13}C NMR study on conformation and dynamics of the transmembrane alpha- helices, loops, and C-terminus of [3-^{13}C]Ala-labeled bacteriorhodopsin. *Biochemistry* **33**, 15046–15052
36. Tanio, M., Inoue, S., Yokota, K., Seki, T , Tuzi, S., Needleman, R , Lanyi, J.K., Naito, A., and Saitô, H (1999) Long-distance effects of site-directed mutations on backbone conformation in bacteriorhodopsin from solid state NMR of [1-^{13}C]Val-labeled proteins *Biophys. J.* **77**, 431–442
37 Torchia, D.A. and Lyerla, J.Jr. (1974) Molecular mobility of polypeptides containing proline as determined by ^{13}C magnetic resonance. *Biopolymers* **13**, 97–114
38. Wishart, D S., Sykes, B.D., and Richards, F.M. (1991) Relationship between nuclear magnetic resonance chemical shift and protein secondary structure. *J. Mol Biol* **222**, 311–333
39 Booth, P.J and Farooq, A. (1997) Intermediates in the assembly of bacteriorhodopsin investigated by time-resolved absorption spectroscopy *Eur J. Biochem.* **246**, 674–680
40 Tuzi, S., Naito, A., and Saitô, H (1996) Temperature-dependent conformational change of bacteriorhodopsin as studied by solid-state ^{13}C NMR. *Eur. J. Biochem.* **239**, 294–301
41. Ebrey, T.G , Becher, B , Mao, B , and Kilbride, P. (1977) Exciton interactions and chromophore orientation in the purple membrane. *J. Mol Biol* **112**, 377–397
42. Heyn, M P , Bauer, P-J , and Dencher, N.A. (1975) A natural CD label to probe the structure of the purple membranes of exciton coupling effects. *Biochem. Biophys. Res. Commun.* **67**, 897–903
43. Krebs, M P , Li, W., and Halambeck, T.P. (1997) Intramembrane substitutions in helix D of bacteriorhodopsin disrupt the purple membrane. *J Mol. Biol.* **267**, 172–183
44 Isenbarger, T.A. and Krebs, M P (1999) Role of helix-helix interaction in assembly of the bacteriorhodopsin lattice. *Biochemstry* **38**, 9023–9030
45. Kataoka, M., Kamikubo, H , Tokunaga, F , Brown, L.S., Yamazaki, Y , Maeda, A., Sheves, M , Needleman, R., and Lanyi, J K. (1994) Energy coupling in an ion pump. The reprotonation switch of bacteriorhodopsin. *J Mol. Biol* **243**, 621–638
46 Brown, L.S , Kamikubo, H , Zimanyi, L , Kataoka, M., Tokunaga, F , Verdegem, P., Lugtenburg, J , and Lanyi, J.K. (1997) A local electrostatic change is the cause of the large-scale protein conformation shift in bacteriorhodopsin. *Proc. Natl. Acad. Sci USA* **94**, 5040–5044
47 Kimura, S., Naito, A., Tuzi, S , and Saitô, H. (2000) A ^{13}C NMR study on [3-^{13}C]-, [1-^{13}C]Ala- or [1-^{13}C]Val-labeled transmembrane peptides of bacteriorhodopsin in in lipid bilayers: insertion, rigid-body motions and local conformational fluctuation at ambient temperature, *Biopolymers*, submitted.
48. Israelewitz, B , Izrailev, S., and Schulten, K. (1997) Binding pathway of retinal to bacterio-opsin: a prediction by molecular dynamics simulations. *Biophys. J.* **73**, 2972–2979